Journal of Applied Fluid Mechanics, Vol. 10, No. 5, pp. 1235-1246, 2017.
Available online at www.jafmonline.net, ISSN 1735-3572, EISSN 1735-3645.
DOI: 10.18869/acadpub.jafm.73.242.26605

Evaluation of Optimum Modes and Conditions of Cavitation and Acoustic Absorption Intensification for Increasing Efficiency of Gas Mixtures Separation

R. N. Golykh

Biysk Technological Institute (branch) of Altai State Technical University named after I.I. Polzunov, Biysk, Altai Region, 659305, Russia

Email: romangl90@gmail.com

(Received May 31, 2016; accepted April 18, 2017)

ABSTRACT

The paper presents theoretical studies of absorption gas mixture separation under ultrasonic vibrations influence, which provides cavitation and acoustic process intensification. The theoretical studies based on consecutive consideration of this process beginning with single cavitation bubble dynamic which generates shockwave for increasing interface "gas-liquid" and ending with determining absorption productivity providing required concentration of target gas mixture component. In result of the studies, it is evaluated, that cavitation and acoustic intensification increase interface "gas-liquid" up to 3 times with amplitude of oscillations of solid surface 1…2 μm. From the data about surface increasing the analysis of the gas absorption process in the liquid film was performed. For this analysis, the model of gas absorption taking into account surface increasing under acoustic cavitation influence was developed. The model of absorption allows to obtain that the absorption productivity under ultrasonic vibrations influence is increased up to 2 times and more. The obtained results can be used for development of high-efficiency absorption apparatus that is supplemented by ultrasonic influence sources.

Keywords: Absorption; Cavitation; Gas mixture; Ultrasonic; Interphase surface.

NOMENCLATURE

A	amplitude of ultrasonic action
A_{ij}	i, j-th component of the matrix of linear system
a	radius of the cavitation bubble at maximum pressure in the nucleus
b	instantaneous distance between the center of the cavitation bubble and the solid surface
b_0	distance (at maximum bubble expansion) between bubble center and solid surface
b_i	i-th component of vector of right part of linear equations system
C	concentration of absorbed gaseous component in liquid film
C_g	concentration of absorbed gaseous component in gas mixture
C_{g0}	initial concentration of absorbed gaseous component in gas mixture
C_{gout}	concentration of absorbed gaseous component at output
c	local velocity of sound in liquid phase
D	coefficient of gaseous component mass transfer into liquid film
$\mathbf{d}_{ij}$	vector of center line of i-th and j-th bubbles couple, which equals $\mathbf{d}_{ij}=\mathbf{r}_j-\mathbf{r}_i$
$E_{r_0}(\mathbf{r})$	fundamental solution of Laplace's equation
f	frequency of ultrasonic action
h	thickness of liquid film
I, I_0, J	integrals over on each boundary item
i	average number of cavitation bubble pulsation before its collapse
j	mean amount of the nuclei generated at the breakage of the separate bubble
K	mean curvature of the walls of the cavitation bubble
K_P	relative absorption productivity increasing under ultrasonic influence
K_S	relative interphase area square increasing under ultrasonic influence
k_B	constant of coalescence rate of the bubbles
L	length of the model area of absorption process
l	norm of difference vectors $\mathbf{r}_1$ and $\mathbf{r}_2$
l_0	norm of vector $\mathbf{r}_0$

$\mathbf{l}_{0\alpha}$, $\mathbf{l}_{\alpha}$	vectors which are depended on α
l_1	norm of vector $\mathbf{r}_1$
N	count of boundary items
n	number concentration of cavitation bubbles depending on time t
$\mathbf{n}$	vector of normal
n_0	initial unknown concentration of cavitation bubbles
n_∞	stationary concentration of cavitation bubbles
p	instantaneous value of pressure of liquid phase without cavitation bubbles
p_0	static pressure in liquid
$p_c(t_1)$	pressure in the nucleus of the cavitation bubble
p_V	pressure of saturated vapor of liquid
p_{wi}	gas pressure near the walls of i-th bubble
R	instantaneous radius of the cavitation bubble
R_0	radius of cavitation nucleus
R_{0i}	radius of i-th bubble nucleus
R_i	instantaneous radius of i-th bubble
R_{MAX}	maximum radius of the bubble
$\mathbf{r}$, $\mathbf{r}_0$, $\mathbf{r}_1$, $\mathbf{r}_2$	vectors of coordinates of the points of the wall of the cavitation bubble
$\mathbf{r}_i$	coordinate vector of the center of i-bubble
S	specific area of the interface
S_A	wall of the cavitation bubble
S_B	solid surface on which $V_{\mathbf{n}}$ is equal 0
S_{eff}	square of effective bubbles collision's cross-section which is proportional to R_{MAX}^2
T_0	period of ultrasonic vibrations
t, t_1	moments of time
u	velocity of liquid film motion
$<u>$	approach velocity of the cavitation bubbles
u_g	velocity of gaseous mixture motion
$V_{\mathbf{n}}$	normal component of fluid velocity
V	volume of the cavitation bubble
$V_n^{(i)}$	normal velocity on i-th bubble wall boundary item with coordinates $(r_i; z_i)$ and $(r_{i+1}; z_{i+1})$
$V_{\boldsymbol{\tau}}$	tangential component of fluid velocity
v_L	instantaneous vibrational speed of liquid phase without cavitation bubbles
λ	length of the capillary wave defined from the condition
α	azimuth angle
γ	adiabatic index of saturated liquid vapor
μ	dynamic viscosity of liquid
$\xi(\mathbf{r}, t)$	value of displacement of the interface "liquid-gas" along the axis
ρ	density of liquid
ρ_L	density of liquid phase
ρ_G	equilibrium density of gas inside the bubble
σ	liquid surface tension
φ	fluid velocity potential on the wall of the cavitation bubble or solid surface
ω	circular vibration frequency of solid surface

1. INTRODUCTION

The problem of artificial separation of gas mixtures caused by the rapid development of techniques and technologies is for over 100 years (Mulder 1996). Until today, in connection with the development of production, technology, transportation and medicine, demand for the separation of gas mixtures for separation of finished products, and to remove undesirable impurities, is constantly growing.

One good example is the increasing demand for chemically pure hydrogen. Today, due to avalanche increase in the number of exhaust gases emitted into the atmosphere, in fact it is necessary to organize a network of hydrogen filling stations to carry out a wide spread of environmentally friendly kinds of autos. Obviously, this will require a manifold increase in the hydrogen production volumes to values which are comparable with today's volumes of produced fossil fuels based on crude oil and natural gas. In this case, it is necessary to provide a low cost of the product. It naturally follows the need to create high-performance and low-cost gas separation plants, because as the primary method of hydrogen production is steam reforming of natural gas/methane (Rostrup-Nielsen and Sehested 2003). The steam reforming results a gaseous mixture of H2, CO2, CH4, H2O and CO, from which it is necessary to separate the H2 only.

Another example is the growing need for oxygen regeneration from CO2 to organize underwater expeditions and long manned space flight to study extraterrestrial objects. The life support systems for such flights and expeditions need high performance, cost-effective and compact device for the O2. In one way or another, the process will be reduced to the separation of oxygen from a mixture of carbon compounds (Konikoff, 1961). High demand on the performance and efficiency of these systems is due to the need for the greatest possible number of crew and severe restrictions on the amount of energy produced on board the spacecraft or submarine vessels.

You can lead a lot of other examples that show the need to increase productivity and reduce energy gas separation mixture. However, despite the breadth of application of the separation of gas mixtures in a variety of spheres of human activity, and at the same time high energy efficient gas separation processes to date does not exist.

Existing devices for gas separation based on

cryogenic, membrane, and sorption methods (Mulder 1996; McNeil *et al.* 2000; Ho *et al.* 2008; Scholes 2013; Amin *et al.* 2014) have limited capacity and are now working virtually at maximum capacity.

The potential effectiveness of the cryogenic and membrane separation technology gases today can be considered as exhausted. For cryogenic technologies it is true because of a long start-up period and the need to cool the gas mixture to the boiling point of the lowest boiling point component, for the membrane technologies it is true due to the high compressed gas flow resistance of the membrane.

Thus, today, it is the most promising division sorption methods (Ho *et al.* 2008; Laugier *et al.* 2008; Scholes *et al.* 2013). Among sorption methods the gaseous absorption by special absorbing liquid has the greatest practical interest. The absorption performance can be up to 200 000 m^3/h due to the fact that the absorption of the gas component occurs by the all volume of the absorbing liquid. However, due to increasing demands in the gas mixture separation, today this performance is insufficient. Attempts to improve the performance of absorption by increasing the absorbent flow rate is a liquid leads to a disproportionate increasing the cost of the process due to the high cost of the regeneration of the absorbent. Increasing of the flow of the gas mixture obviously leads to decrease the purity of the gases due to limited diffusion rate.

Therefore, one of the possible ways to increase the absorption capacity is the use of external influence leading to increase the interface "liquid-gas" that leads to increase gas absorption rate. Known absorbers is base on creating of the larger interface area using spray absorbing liquid (atomizing absorbers), eg, patent RU 2,380,143 by Znyatdinova *et al.* (2010). However, in this case, gases that are little soluble in the absorbent is practically not absorbed due to occurrence of turbulent micropulsations. Thus, the effectiveness of atomizing absorbers for these gases is reduced to nothing.

Therefore, to solve this problem, it is encouraged by applying of acoustic (ultrasonic) cavitation, the impact of which increases the interfacial surface of the "liquid-gas" (Laugier *et al*. 2008). The acoustic and cavitation influence is effective for the intensification of the processes of absorption that is experimentally proven by domestic and foreign researchers. Acoustic cavitation influence has the following advantages:

1. The possibility of intensification of absorption, regardless of chemical composition of the separated gas and liquid absorbents due to the possibility of choose of the optimal ultrasonic influence mode and exposure conditions (frequency, intensity, location, and direction of the input of ultrasonic vibrations, radiating area) determined by the physical properties of gaseous mixture and absorbing liquid.

2. Installation of ultrasound sources does not require changes in the design and functionality of the absorbers.

3. Low power consumption. According to the results of laboratory tests, the intensification of gas absorption occurs even at low intensity exposure, if you select a certain resonance frequency of the oscillation.

4. The possibility of simultaneous intensification of chemisorption because cavitation contribute to breakage of chemical bonds and the formation of new ones.

5. Compact sources of ultrasonic vibrations and electronic generators for their power.

However, despite a number of advantages, in practice, today the acoustic cavitation effects is not been implemented due to lack of knowledge of the physical mechanisms of the process and the lack of scientific data of the best modes of ultrasonic action providing maximum efficiency of the process as consequence.

Due to time consuming and expensive experimental studies it is necessary to develop a mathematical model of the effect of ultrasonic influence on the interfacial surface area of the "liquid-gas" and the kinetics of absorption, allowing evaluating optimal modes of acoustic cavitation intensification of this process.

2. PROBLEM STATEMENT

According to the method of acoustic cavitation intensification of absorption (Fig. 1), into the thin liquid film (absorbent) powerful acoustic or ultrasonic (US) oscillations (frequency of 20...250 kHz) is introduced by solid-state transmitter (Khmelev *et al.* 2012; Laugier *et al.* 2008).

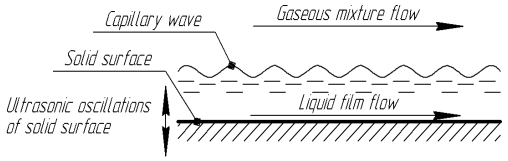

Fig. 1. Scheme of the acoustic cavitation intensification of absorption.

Ultrasonic vibrations in fluid create acoustic cavitation field (Rozenberg 1968; Khmelev 2011). It is the cavitation bubbles, which periodically expand and collapse into non-spherical nuclei (non-spherical shape is caused by solid surface) forming microscopic shockwaves with pressure pulses up to 1000 atmospheres (Fig. 2) (Rozenberg 1968; Kedrinsky 2000; Brennen 1995; Ruckenstein and Nowakowski 1990; Malagetti *et al.* 2015a). Shock waves lead to the formation of stable capillary waves on the interface "liquid-gas" (Khmelev *et al.* 2012), which allows to increase the area of the

interface and hence speed of separation of gas mixtures.

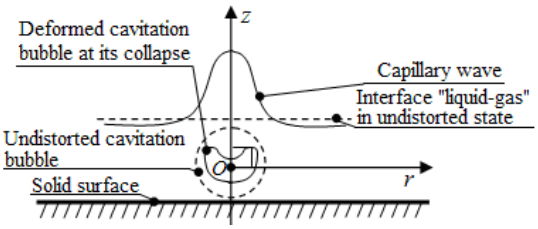

Fig. 2. Scheme of the capillary wave formation under influence of cavitation bubble.

Thus, the model to identify optimal modes of acoustic absorption intensification should include the following stages of the process review (Khmelev *et al.* 2014b):

1. expansion of cavitation bubble up to maximum radius, which is spherically symmetric due to the low speed of its walls (no more than 15 m/s);
2. asymmetric collapse (Malagetti *et al.* 2015b, 2016) of the cavitation bubble from maximum radius to minimum size;
3. generation and propagation of narrow directional shock wave in the thin liquid film at the collapse of the cavitation bubble;
4. formation of capillary waves on interface "liquid-gas". In this stage capillary waves profile is determined and square of the interface "liquid-gas" is calculated;
5. absorption of gaseous mixture flow component by liquid film. In this stage the absorption productivity providing the necessary purity of target component is determined.

Further proposed model is described.

3. The Model Of Acoustic Cavitation Intensification Of Absorption

3.1 Expansion of Cavitation Bubble

At the stage of cavitation bubble expansion its maximum radius R_{MAX} and center z location relative to the solid surface are determined. At this stage it is assumed that:

1. expansion of the bubble is spherically symmetric, which is caused by low speed of walls motion, however the bubble center vertically moves relative to the solid surface in the course of time;
2. in initial time the center of the cavitation bubble is located near the solid surface, as such bubbles mostly influence on the formation of capillary wave.

Maximum radius of the bubble R_{MAX} is defined on the base of Nolting-Neppiras equation (Rozenberg 1968):

$$\rho\left(\frac{3}{2}\left(\frac{\partial R}{\partial t}\right)^2 + R\frac{\partial^2 R}{\partial t^2}\right) = \\ = -4\mu\frac{\frac{\partial R}{\partial t}}{R} + p_V + \left(p_0 + \frac{2\sigma}{R_0}\right)\left(\frac{R_0}{R}\right)^{3\gamma} - \\ - p_0 + 4\pi^2 f^2 \rho A h \sin(2\pi f t) \tag{1}$$

where R is the instantaneous radius of the cavitation bubble, m; R_0 is the radius of cavitation nucleus, m; σ is the liquid surface tension, N/m; ρ is the density of liquid, kg/m^3; p_0 is the static pressure in liquid, Pa; f is the frequency of ultrasonic action, Hz; h is the thickness of liquid film, m; A is the amplitude of ultrasonic action, m; pv is the pressure of saturated vapor of liquid, Pa; t is the time, s; μ is the dynamic viscosity of liquid, Pa·s.

The distance between the center of the cavitation bubble (at the moment of maximum expansion) and the solid surface is defined from the equation given in Rozhdestvenskiy's book (1977):

$$6b^2\frac{\partial b}{\partial t}\frac{\partial R}{\partial t} + 2b^2 R\frac{\partial^2 b}{\partial t^2} + 3R^2\left(\frac{\partial R}{\partial t}\right)^2 = 0 \tag{2}$$

where b is the distance between the center of the cavitation bubble and the solid surface, m.

Obtained values of maximum bubble radius and the distance between its center and the solid surface are used for theoretical studies of further stages of the capillary wave formation.

3.2 Collapse of Cavitation Bubble

During the study of the stage of cavitation bubble collapse its form in the moment of the minimum size is determined.

The form of the cavitation bubble is defined from the integral equation (3) with boundary conditions (4, 5) on the wall of the cavitation bubble for liquid velocity potential and entry conditions (6, 7) on cavitation bubble wall:

$$\frac{\varphi(\mathbf{r}_0)}{2} = \int\limits_{S_A \cup S_B}\left(E_{\mathbf{r}_0} V_{\mathbf{n}} - \frac{\partial E_{\mathbf{r}_0}}{\partial \mathbf{n}}\varphi\right)\partial S \tag{3}$$

$$\frac{\partial \varphi}{\partial t} + \frac{|V_{\mathbf{n}}|^2 + |V_{\tau}|^2}{2} = \\ = \frac{2\sigma K}{\rho} - \frac{p_V}{\rho}\left(\frac{3V}{4\pi R_{MAX}^3}\right)^{\gamma} \tag{4}$$

$$\nabla\varphi = \frac{\partial \mathbf{r}}{\partial t} \tag{5}$$

$$\varphi|_{t=0} = 0 \tag{6}$$

$$|\mathbf{r}|_{t=0} = R_{MAX} \tag{7}$$

where $\mathbf{r}_0$, $\mathbf{r}$ are the vectors of the coordinates of the points of the wall of the cavitation bubble or solid surface, m; φ is the fluid velocity potential on the

wall of the cavitation bubble or solid surface, m^2/s; $V_{\mathbf{n}}$ and $V_{\boldsymbol{\tau}}$ are the normal and tangential components of fluid velocity, m/s; $E_{r_0}(\mathbf{r})$ is the fundamental solution of Laplace's equation; V is the volume of the cavitation bubble, m^3; p_V is the pressure of saturated vapor of fluid, Pa; ρ and σ are the density (kg/m^3) and surface tension (N/m) of fluid, respectively; K is the mean curvature of the walls of the cavitation bubble, m^{-1}; S_A is the wall of the cavitation bubble; S_B is the solid surface on which $V_{\boldsymbol{n}}$ is equal 0 (See Fig. 2).

With the help of system of equations (3-7) we calculate deformation of the walls of the cavitation bubble in the course of time. Entry conditions (5-7) being a part of the system (3-7) is determined by the bubble radius and the position of its center at the moment of maximum expansion, which were found at the previous stage of the model study. Integral equation (3) aimed at the determination of distribution of fluid velocity potential on the walls of the cavitation bubble is solved by the boundary element method. For this purpose the discretization of the cavitation bubble wall into ring elements is carried out, as it is shown in Fig. 3.

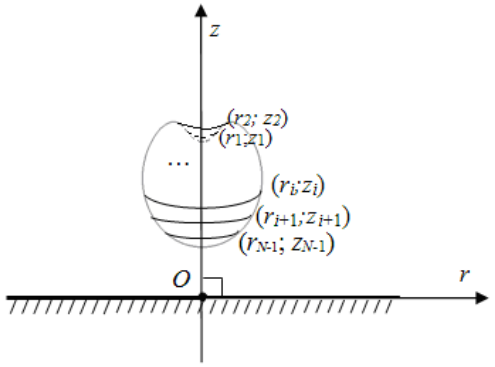

Fig. 3. Discretization of the cavitation bubble wall into ring boundary elements.

It is assumed, that in the frameworks of each ring element the velocity potential is constant. It allows solving boundary integral equation (3) as a system of linear equations (8). This system is obtained by using method of "images" (replacing solid surface by symmetrically placed cavitation bubble).

$$\left\{A_{ij}\right\}_{i,j=1\ldots 2N}\begin{Bmatrix} V_n^{(1)} \\ V_n^{(2)} \\ \ldots \\ V_n^{(N-1)} \\ V_n^{(N)} \\ V_n^{(1)} \\ V_n^{(2)} \\ \ldots \\ V_n^{(N-1)} \\ V_n^{(N)} \end{Bmatrix} = \left\{b_i\right\}_{i=1\ldots 2N} \tag{8}$$

where $\{A_{ij}\}$ is the matrix of linear system; $V_n^{(i)}$ is normal velocity on i-th bubble wall boundary item with coordinates (r_i; z_i) and (r_{i+1}; z_{i+1}); $\{b_i\}$ is right part of system; N is count of boundary items;

The coefficients of the system of linear equations (A_{ij} and b_i) are defined by the following obtained expressions:

$$b_{i+pN} = \frac{\varphi_{\max(i-1;1)} + \varphi_{\min(i,N-1)}}{2}\left[\frac{1}{2} + J\left(\begin{pmatrix} r_{i-1} \\ (2p-1)z_{i-1} - (1-p)b_0 \end{pmatrix}, \begin{pmatrix} r_i \\ (2p-1)z_i - (1-p)b_0 \end{pmatrix}, \frac{\begin{pmatrix} r_i + r_{i-1} \\ (1-2p)(z_i + z_{i-1}) - pb_0 \end{pmatrix}}{2}, \frac{\begin{pmatrix} z_{i-1} - z_i \\ (2p-1)(r_i - r_{i-1}) \end{pmatrix}}{\sqrt{(r_i - r_{i-1})^2 + (z_i - z_{i-1})^2}}\right)\right] +$$

$$+ \sum_{q=0}^{1}\sum_{j=1,\, j+qN\neq i+pN}^{N} \frac{\varphi_{\max(j-1;1)} + \varphi_{\min(j,N-1)}}{2} \times$$

$$\times J\left(\begin{pmatrix} r_{j-1} \\ (1-2q)z_{j-1} - qb_0 \end{pmatrix}, \begin{pmatrix} r_j \\ (1-2q)z_j - qb_0 \end{pmatrix}, \frac{\begin{pmatrix} r_i + r_{i-1} \\ (1-2p)(z_i + z_{i-1}) - pb_0 \end{pmatrix}}{2}, \frac{\begin{pmatrix} z_{j-1} - z_j \\ (1-2q)(r_j - r_{j-1}) \end{pmatrix}}{\sqrt{(r_j - r_{j-1})^2 + (z_j - z_{j-1})^2}}\right) \tag{9}$$

$$\left\{A_{(i+pN)(j+qN)}\right\} = \delta_{ij}\delta_{pq} \times$$

$$\times I_0\left(\begin{pmatrix} r_{j-1} \\ z_{j-1} - q(b_0 + 2z_{j-1}) \end{pmatrix}, \begin{pmatrix} r_j \\ z_j - q(b_0 + 2z_j) \end{pmatrix}\right) +$$

$$+ (1 - \delta_{ij}\delta_{pq}) \times \tag{10}$$

$$\times I\left(\begin{pmatrix} r_{j-1} \\ (1-2q)z_{j-1} - qb_0 \end{pmatrix}, \begin{pmatrix} r_j \\ (1-2q)z_j - qb_0 \end{pmatrix}, \frac{1}{2}\begin{pmatrix} r_i + r_{i-1} \\ (1-2p)(z_i + z_{i-1}) - pb_0 \end{pmatrix}\right)$$

where I_0, J, I are integrals over on each boundary item; b_0 is distance between bubble center and solid surface at maximum bubble expansion, m.

In expressions (9-10) it is mentioned that following equalities are true:

$$\begin{pmatrix} r_0 \\ z_0 \end{pmatrix} = \begin{pmatrix} r_1 \\ z_1 \end{pmatrix}; \quad \begin{pmatrix} r_N \\ z_N \end{pmatrix} = \begin{pmatrix} r_{N-1} \\ z_{N-1} \end{pmatrix}.$$

Integrals I_0, J, I are defined as follows (11-13):

$$J(\mathbf{r}_1, \mathbf{r}_2, \mathbf{r}_0, \mathbf{n}) = \int_0^{2\pi} \left([r_1 - r_0 \cos\alpha] n_r + (z_1 - z_0) n_z \right) \times \left(\left. \frac{-\frac{r_2 - r_1}{4\pi l^2}}{\sqrt{t^2 + k_\alpha{}^2}} \right|_{t=\frac{(\mathbf{r}_1 - \mathbf{l}_\alpha, \mathbf{l})}{l^2}}^{t=1+\frac{(\mathbf{r}_1 - \mathbf{l}_\alpha, \mathbf{l})}{l^2}} + \right.$$
$$\left. + \frac{r_1 - \frac{(\mathbf{r}_1 - \mathbf{l}_\alpha, \mathbf{l})}{l^2}(r_2 - r_1)}{4\pi l^2 k_\alpha{}^2} \times \left. \frac{t}{\sqrt{t^2 + k_\alpha{}^2}} \right|_{t=\frac{(\mathbf{r}_1 - \mathbf{l}_\alpha, \mathbf{l})}{l^2}}^{t=1+\frac{(\mathbf{r}_1 - \mathbf{l}_\alpha, \mathbf{l})}{l^2}} \right) \partial\alpha \qquad (11)$$

$$I(\mathbf{r}_1, \mathbf{r}_2, \mathbf{r}_0) = -\frac{1}{4\pi} \times \int_0^{2\pi} \left(\ln \left| \frac{l_{1\alpha} + l + \frac{(\mathbf{l}_1 - \mathbf{l}_\alpha, \mathbf{l})}{l}}{\sqrt{|\mathbf{l}_1 - \mathbf{l}_\alpha|^2} + \left(\mathbf{l}_1 - \mathbf{l}_\alpha, \frac{\mathbf{l}}{l}\right)} \right| \times \left(r_1 - (r_2 - r_1) \frac{(\mathbf{l}_1 - \mathbf{l}_\alpha, \mathbf{l})}{l^2} \right) + \right.$$
$$\left. + (r_2 - r_1) \left(\frac{l_{1\alpha}}{l} - \frac{|\mathbf{l}_1 - \mathbf{l}_\alpha|}{l} \right) \right) \partial\alpha \qquad (12)$$

$$I_0(\mathbf{r}_1, \mathbf{r}_2) = -\frac{1}{2\pi} \times \lim_{\varepsilon \to 0+} \int_\varepsilon^\pi \left(\ln \left| \frac{l k_{0\alpha}{}^2 + l + \frac{(\mathbf{r}_1 - \mathbf{l}_{0\alpha}, \mathbf{l})}{l}}{\sqrt{|\mathbf{r}_1 - \mathbf{l}_{0\alpha}|^2} + \left(\mathbf{r}_1 - \mathbf{l}_{0\alpha}, \frac{\mathbf{l}}{l}\right)} \right| \times \left(r_1 - (r_2 - r_1) \frac{(\mathbf{r}_1 - \mathbf{l}_{0\alpha}, \mathbf{l})}{l^2} \right) + \right.$$
$$\left. + (r_2 - r_1) \left(k_{0\alpha}{}^2 - \frac{|\mathbf{r}_1 - \mathbf{l}_{0\alpha}|}{l} \right) \right) \partial\alpha \qquad (13)$$

$$k_{0\alpha}{}^2 = \frac{|\mathbf{r}_1 - \mathbf{l}_{0\alpha}|^2 + l^2 + 2(\mathbf{r}_1 - \mathbf{l}_{0\alpha}, \mathbf{l})}{l^2}$$

$$k_\alpha{}^2 = -\frac{(\mathbf{r}_1 - \mathbf{l}_\alpha, \mathbf{l})^2}{l^4} + \frac{l_1{}^2 + l_0{}^2 - 2(\mathbf{r}_1, \mathbf{l}_\alpha)}{l^2}$$

$$l_{1\alpha} = \sqrt{|\mathbf{l}_1 - \mathbf{l}_\alpha|^2 + l^2 + 2(\mathbf{l}_1 - \mathbf{l}_\alpha, \mathbf{l})}$$

where r_1, r_2, r_0 are vectors of coordinates $\mathbf{r}_1 = \begin{pmatrix} r_1 \\ z_1 \end{pmatrix}; \mathbf{r}_2 = \begin{pmatrix} r_2 \\ z_2 \end{pmatrix}; \mathbf{r}_0 = \begin{pmatrix} r_0 \\ z_0 \end{pmatrix}$; $\mathbf{n}$ is vector of normal $\mathbf{n} = \begin{pmatrix} n_r \\ n_z \end{pmatrix}$; $\mathbf{l}_\alpha = \begin{pmatrix} r_0 \cos\alpha \\ z_0 \end{pmatrix}$;

$$\mathbf{l}_{0\alpha} = \frac{1}{2} \begin{pmatrix} (r_1 + r_2)\cos\alpha \\ z_1 + z_2 \end{pmatrix};$$

$$l = \sqrt{(r_2 - r_1)^2 + (z_2 - z_1)^2}; \quad l_1 = \sqrt{r_1{}^2 + z_1{}^2}; \quad l_0 = \sqrt{r_0{}^2 + z_0{}^2}.$$

Obtained system of linear equations (8) is solved by iterative Seidel method.

Obtained forms of cavitation bubble walls (by equations (3-7) at the collapse in different moments of time are shown in Fig. 4. The initial moment of time (0 μs) is the moment of the maximum bubble expansion.

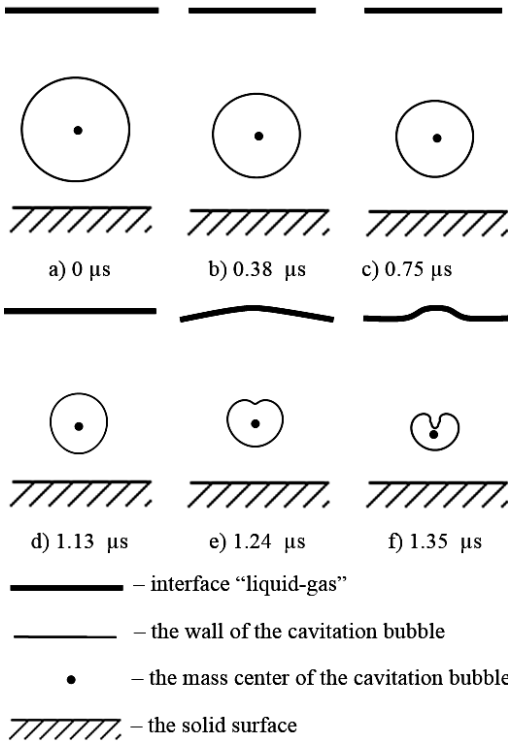

Fig. 4. Shapes of cavitation bubble at different times.

As it is shown in Fig. 4, cavitation bubble likes a hemispherical radiator of shock wave.

The shape and size of cavitation bubble obtained at the collapse are input data for study of generation and propagation of shock wave.

3.3 Generation and Propagation of Shock Wave

At the study of the stages of generation and propagation of shock wave it allows approximating its pressure profile at different distances from the

bubble by the following obtained expression (14).

$$p(\mathbf{r},t) = -\sum_{n=-\infty}^{\infty} \frac{\omega}{2\pi} a\varepsilon \times$$
$$\times \mathrm{Re}\left[\int_0^{\frac{\pi}{2}} \int_0^{\frac{2\pi}{\omega}} p_c(t_1) e^{\frac{i\omega n}{c}\left(c(t-t_1) + \frac{a}{\varepsilon} - \frac{\mu n \omega}{2\rho c^2} + z\varepsilon\cos\psi \right)} \times \right. \quad ; \quad (14)$$
$$\left. \times \sin\psi \frac{in\omega}{2\pi c} \int_0^{2\pi} \cos\left(n \frac{\omega r \varepsilon \sin\psi}{c} \sin(\beta) \right) \partial\beta \partial t_1 \partial\psi \right]$$

$$\varepsilon = \frac{a}{\sqrt{r^2 + z^2}};$$

where $(r; z)$ are the coordinates of the points, m; ω is the circular vibration frequency of solid surface, s^{-1}; t and t_1 are the moments of time, s; μ is the viscosity of liquid, Pa·s; ρ and c is the velocity of sound in liquid, m/s; $p_c(t_1)$ is the pressure in the nucleus of the cavitation bubble, Pa; a is the radius of the cavitation bubble at maximum pressure in the nucleus, m.

The function of shock wave pressure in the nucleus of the cavitation bubble $p_c(t_1)$ being a part of the expression (14) is defined as:

$$p_c(t_1) = p_V \left(\frac{4\pi R_{MAX}^3}{3V} \right)^{\gamma};$$

where p_V is pressure of saturated liquid vapor; R_{MAX} is bubble radius at maximum expansion; V is bubble volume at time t_1; γ is a adiabatic index of saturated liquid vapor.

Given profile of shock wave pressure is used further for the definition of capillary wave form and finally interphase boundary area.

3.4 Formation of Capillary Waves on Surface "Liquid-Gas"

The form of the single capillary wave is defined from the expression (15):

$$\xi(r,t) = -\frac{1}{\rho} \int_0^t \int_0^{t_2} \frac{\partial p}{\partial z} \partial t_1 \partial t_2 \quad (15)$$

where $\xi(r,t)$ is the value of displacement of the interface "liquid-gas" along the axis z.

However at the realization of the technological process it is impossible to obtain separate bubble that is why it is necessary to consider the interaction between the aggregate of cavitation bubbles and the interface generating set of capillary waves.

The specific area of the interface "liquid-gas" per unit volume of liquid phase at the generation of the set of capillary waves is defined by the expression (16):

$$S = 2\pi \langle n \rangle \int_0^{0,5\lambda} r \sqrt{1 + \left(\frac{\partial \xi}{\partial r} \right)^2} \partial r + \frac{1}{h} \quad (16)$$

where S is the specific area of the interface, m^2/m^3; λ is the length of the capillary wave (m) defined from the condition $\frac{\partial \xi}{\partial r}\left(\frac{\lambda}{2}, t\right) = 0$; n is the concentration of cavitation bubbles, m^{-3}; $< >$ is sign of averaging by liquid film thickness; h is thickness of liquid film, m.

The term $2\pi \langle n \rangle \int_0^{0,5\lambda} r \sqrt{1 + \left(\frac{\partial \xi}{\partial r} \right)^2} \partial r$ characterizes a shock wave energy being generated at bubble collapse.

For the concentration of cavitation bubbles kinetic equation (17) obtained from Smolukhovskiy's equation (Sheng and Shen 2006) for the processes of coalescence and breakage of disperse particles (liquid drops, gas and solid particles) is true (Margulis 2007):

$$\frac{\partial n}{\partial t} = \frac{n(j-1)}{iT_0} - k_B n^2 \quad (17)$$

where n is the calculating concentration of cavitation bubbles depending on time t, m^{-3}; i is the average number of cavitation bubble pulsation before its collapse; k_B is the constant of coalescence rate of the bubbles, m^3/s; T_0 is the period of ultrasonic vibrations, s; j is the mean amount of the nuclei generated at the breakage of the separate bubble.

By solving the equation (17) following analytic expression is obtained:

$$n = \frac{n_\infty n_0}{n_0 + (n_\infty - n_0) e^{-n_\infty k_B t}}; \quad (18)$$

where n_0 is the initial unknown concentration of cavitation bubbles, m^{-3}; n_∞ is the stationary concentration of cavitation bubbles, m^{-3}.

According to the expression (18) the concentration of the bubbles n in time, which equals tens periods of ultrasonic vibrations, achieves stable value and equals to n_∞, which is defined by the expression (19):

$$n_\infty = \frac{j-1}{ik_B T_0}; \quad (19)$$

Variable j being in expression for stable concentration (19) is calculated from experimental data given in Rozenberg's book (Rozenberg 1968).

The constant of coalescence is defined as follows:

$$k_B = \frac{S_{eff} \langle u \rangle}{2}; \quad (20)$$

where S_{eff} is square of effective bubbles collision's cross-section which is proportional to R_{MAX}^2, m^2; $<u>$ is approach velocity of the cavitation bubbles, m/s.

To define approach velocity of the cavitation bubbles $<u>$ the model of bubble interaction caused by the forces of the second order is used. The interaction model is based on the 2nd Newton's Law for the separate cavitation bubble

taking into consideration Bjerknes force acting from the neighbor bubbles and caused by radial vibrations of the last ones. According to this model the position of the center of each cavitation bubble making the ensemble can be described by the following equation (Margulis 2007):

$$\frac{4\pi R_{0i}^{\ 3}}{3}\rho_G\frac{\partial^2\mathbf{r}_i}{\partial t^2}=\frac{4\pi R_i^{\ 3}}{3}\rho_L\frac{\partial\mathbf{v}_L}{\partial t}(\mathbf{r}_i,t)+$$
$$+\sum_{j=1,n,j\neq i}\frac{4\pi R_i^{\ 3}}{3|\mathbf{d}_{ij}|^3}\rho_L\frac{\partial\left(R_j^{\ 2}\frac{\partial R_j}{\partial t}\right)}{\partial t}\mathbf{d}_{ij}+ \quad (21)$$
$$+\frac{1}{2}\frac{\partial}{\partial t}\left(\frac{4\pi R_i^{\ 3}}{3}\rho_L\left(\mathbf{v}_L(\mathbf{r}_i,t)-\frac{\partial\mathbf{r}_i}{\partial t}\right)\right)+$$
$$+4\pi\mu R_i\left(\mathbf{v}_L(\mathbf{r}_i,t)-\frac{\partial\mathbf{r}_i}{\partial t}\right)$$

where i is the ordinal number of the bubble in zone of liquid phase; R_i is the instantaneous radius of i-th bubble, m; c is the local velocity of sound in liquid phase, m/s; p_{wi} is the gas pressure near the walls of i-th bubble, Pa; p is the instantaneous value of pressure of liquid phase without cavitation bubbles, Pa; ρ_L is the density of liquid phase, kg/m^3; v_L is the instantaneous vibrational speed of liquid phase without cavitation bubbles, m/s; R_{0i} is the radius of i-th bubble nucleus, m; ρ_G is the equilibrium density of gas inside the bubble, kg/m^3; t is the time, s; μ is the viscosity of liquid phase, Pa·s; $\mathbf{r}_i$ is the coordinate vector of the center of i-th bubble, m; $\mathbf{d}_{ij}=\mathbf{r}_j-\mathbf{r}_i$ is the vector of center line of i-th and j-th bubbles couple, m.

On the base of the results of equation solution (18) approach velocity of cavitation bubbles is defined by the following expression:

$$\langle u\rangle=\frac{|\mathbf{d}_{12}(T_0)-\mathbf{d}_{12}(0)|}{T_0}. \quad (22)$$

Further the approach velocity is substituted in the expression (19), that allows finally to determine the area of the interface "liquid-gas".

Thus, in this stage of model consideration (capillary wave formation) the dependence of surface area of interphase boundary on the modes of ultrasonic action (frequency and vibration amplitude of solid surface covered with liquid film, which borders on gas phase) and liquid properties can be defined. It is follows, this stage allows to define relative square increasing (K_S) under ultrasonic influence:

$$K_S=\frac{S_{US}}{S_{without\ US}}=\frac{2\pi\langle n\rangle\int_0^{0,5\lambda}r\sqrt{1+\left(\frac{\partial\xi}{\partial r}\right)^2}\partial r+\frac{1}{h}}{\frac{1}{h}}= \quad (23)$$
$$=1+2\pi h\langle n\rangle\int_0^{0,5\lambda}r\sqrt{1+\left(\frac{\partial\xi}{\partial r}\right)^2}\partial r$$

Further the relative square increasing is used for calculation of absorption productivity in next stage of model consideration.

3.5 Absorption of Gaseous Mixture Flow Component by Liquid Film

In the stage of model consideration the process is considered according to scheme presented in Fig. 1.

The absorption productivity is defined as maximum productivity providing absorbing component concentration at gaseous mixture output which does not exceed defined value.

For defining of the productivity, the equations of gaseous component diffusion into liquid (24) and mass conservation (25) are used:

$$u\frac{\partial C}{\partial x}=D(C_g-C); \quad (24)$$

$$-u_g\frac{\partial C_g}{\partial x}=u\frac{\partial C}{\partial x}; \quad (25)$$

u is velocity of liquid film motion, m/s; u_g is velocity of gaseous mixture motion, m/s; C is concentration of absorbed gaseous component in liquid film; C_g is concentration of absorbed gaseous component in gas mixture; D is coefficient of gaseous component mass transfer, s^{-1}.

If ultrasound acts on liquid film then coefficient D is multiplied by K_S and the equation (24) is reduced to (26)

$$u\frac{\partial C}{\partial x}=DK_S(C_g-C). \quad (26)$$

The analytical solution of equation systems (24-25) gives the expression (26) for the absorbing gaseous component concentration at output:

$$C_{gout}=C_{g0}\left[\frac{u_g}{u+u_g}+\frac{u}{u+u_g}e^{-DK_S\left(\frac{1}{u_g}+\frac{1}{u}\right)L}\right]; \quad (27)$$

where l is length of the model area of absorption process, m.

It allows to calculate relative increasing K_P of the absorption productivity providing $C_{gout}=\varepsilon C_{g0}$ under ultrasonic vibrations influence (28)

$$K_P=\frac{G_{g2}}{G_{g1}}=\frac{u_{g2}}{u_{g1}}; \quad (28)$$

where G_{g1}, G_{g2} are the required absorbed gaseous mass flows providing concentration $C_{gout}=\varepsilon C_{g0}$ through output without and with US respectively, kg/s; u_{g1}, u_{g2} are the required absorbed gaseous velocities providing concentration $C_{gout}=\varepsilon C_{g0}$ at output without and with US respectively, m/s. The velocities u_{g1}, u_{g2} in expression (28) are determined by the following relation

$$\varepsilon=\frac{u_{g1}}{u+u_{g1}}+\frac{u}{u+u_{g1}}e^{-\frac{D(u+u_{g1})L}{uu_{g1}}}=\frac{u_{g2}}{u+u_{g2}}+\frac{u}{u+u_{g2}}\times$$
$$\times e^{-\frac{DK_S(u+u_{g2})L}{uu_{g2}}}.$$

Thus the stage of model consideration allows to

determine relative absorption productivity increasing under ultrasonic vibrations influence.

In the next section the results obtained by the model analysis is presented.

4. OBTAINED RESULTS

The obtained results contain relative interphase area square and productivity depending on square increasing dependences on ultrasonic influence models and liquid phase properties. Firstly, the relative square increasing under ultrasonic influence dependences were obtained. The dependences are presented in next subsection.

4.1 Relative Increasing of Square

The relative increasing of square is determined by formation of capillary waves on surface "liquid-gas" stage of model consideration.

Obtained dependences of relative increase of the interface area K_S (see expression (23)) on the modes of ultrasonic action are shown in Fig. 5. Fig. 5 shows the breakage of the graph corresponds to the fact, that capillary wave loses its stability and breaks into drops (Khmelev *et al.* 2012). The dependence of frequency (Fig. 5b) is built up at threshold amplitudes, when capillary wave remains stable.

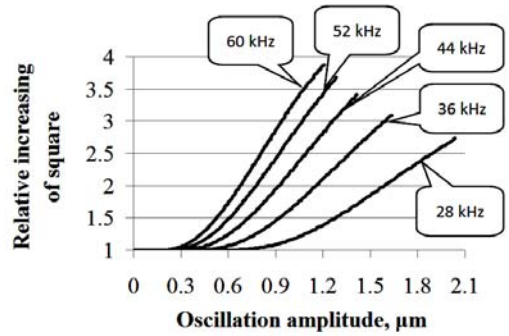

Fig. 5. Dependences of specific area of the interface on the modes of ultrasonic action: (a) on amplitude at different frequencies; (b) frequency at maximum amplitude.

From presented dependences it is evident, that with the increase of amplitude interface area grows. If frequency rises, surface area grows (up to more than 3 times) due to the increase of cavitation bubble concentration (Rozenberg 1968). However starting with the frequency of 60 kHz the growth of the area essentially becomes slower, and energy loss of the ultrasonic radiator increases quadratically. That is why; the application of frequencies of more than 60 kHz is unpractical. Fig. 6 shows the dependence of threshold vibration amplitude, at which capillary wave remains stable, on the frequency of action.

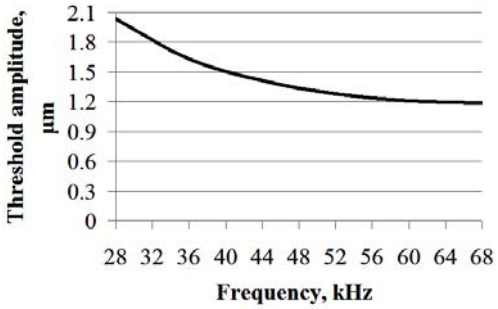

Fig. 6. Dependence of threshold amplitude, at which capillary wave remains stable, on the frequency of action.

According to presented dependence the asymptotic amplitude reduces with the rise of frequency. In particular at the frequency of 28 kHz the threshold amplitude exceeds 2 μm, and at the frequency of 60 kHz it is 1…1.2 μm. Fig. 7 shows the dependences of specific interface area on amplitude at the change of physical properties of liquid – viscosity (a) and surface tension (b), which influence on the profile of contact surface together with the modes of ultrasonic action.

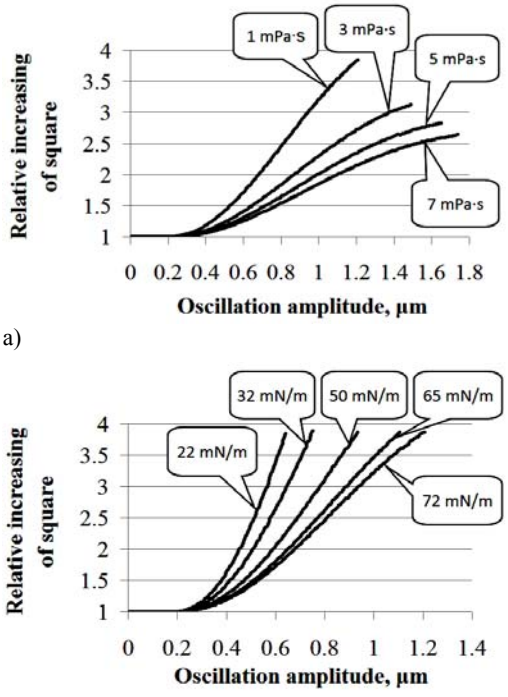

Fig. 7. Dependence of specific area of interphase boundary on amplitude at different properties of liquid (frequency of 60 kHz): viscosity (a) and surface tension (b).

Presented dependences (Fig. 7) can be used for the determination of the area change caused by change of the liquid type and change of its properties. In particular it is stated, that growth of viscosity leads to the decrease specific area of the interface. It is caused by the absorption of energy of shock waves in liquid phase due to forces of viscous friction. At that decrease of surface tension leads to the growth of the area, as surface energy of a liquid directly depends on its surface tension.

Further the dependences are used for calculation of absorption productivity.

4.2 Relative Increasing of Absorption Productivity

The dependences of absorption productivity increasing K_P (See expression (28)) on ultrasonic influence modes (Fig. 8) and liquid properties (Fig. 9) are obtained by absorption of gaseous mixture flow component by liquid film stage of model consideration. The dependences like the dependences of surface area increasing.

The breakage of graphs means a loss of capillary waves stability as well as for relative square increasing dependences.

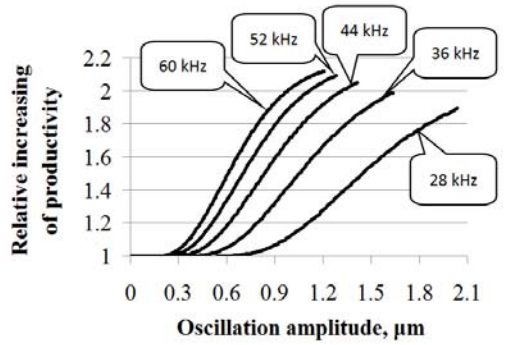

a)

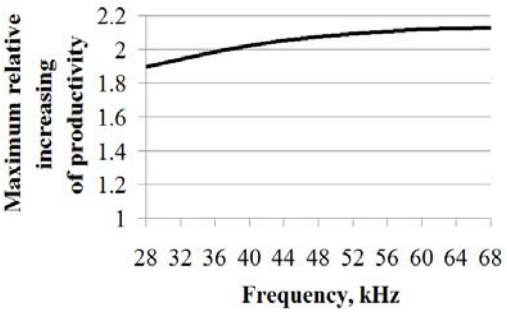

b)

Fig. 8. Dependences of specific area of the interface on the modes of ultrasonic action: (a) on amplitude at different frequencies; (b) on frequency at maximum amplitude.

From presented dependences it is evident, that with the increase of amplitude absorption productivity grows up to more than 2 times.

As well as for the relative square increasing dependences, starting with the frequency of 60 kHz the growth of the maximum productivity essentially becomes slower, and energy loss of the ultrasonic radiator increases quadratically. That is why; the application of frequencies of more than 60 kHz is unpractical.

Presented dependences on amplitude at different liquid properties (Fig. 9) can be used for the determination of the absorption productivity under ultrasonic influence caused by change of the liquid type and change of its properties. In particular it is stated, that growth of viscosity leads to the decreasing productivity or the increasing amplitudes which are necessary to defined productivity achievement, as well as for interface area. At that decrease of surface tension leads to the decreasing amplitudes, which are necessary to defined productivity achievement, and the decreasing maximum amplitude providing capillary waves stability (no breakup into drops).

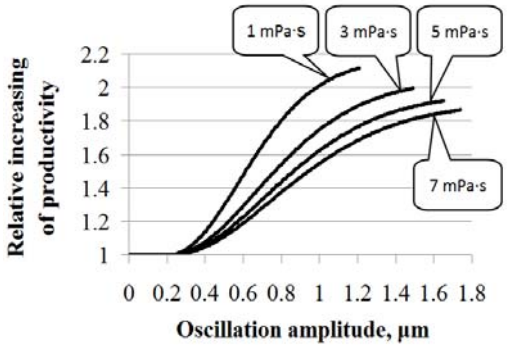

a)

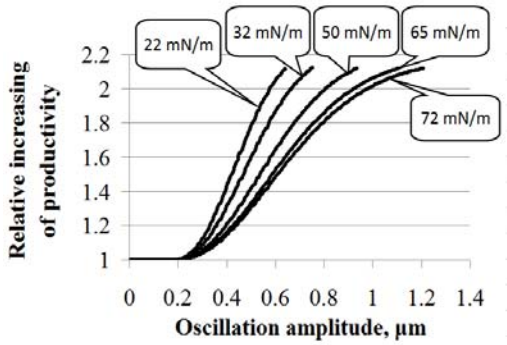

b)

Fig. 9. Dependence of specific area of interphase boundary on amplitude at different properties of liquid (frequency of 60 kHz): viscosity (a) and surface tension (b).

4.3 The Power of US Oscillations Required for Absorption Intensification

Further estimation of power of US oscillations spent for capillary waves formation and absorption intensification was performed. For thin layer of absorbing liquid ($kh << 1$, k is wave number, m^{-1}; h is liquid layer thickness, m) author obtained the expression for specific power of US oscillations (power per unit of layer area I_{cav}, W/m^2) spent for capillary waves formation (29):

$$I_{cav} = C(f)\frac{\rho A^2\omega^4}{2c}\times \\ \times\left(\frac{\rho A^2\omega^4}{10c}\left(h^5 - h_1{}^5\right) - \frac{I_0}{3}\left(h^3 - h_1{}^3\right)\right) \quad (29)$$

For the expression (29) obtaining author assumed that main part of power is transformed to cavitation bubble collapse and oscillations attenuation coefficient (K, m^{-1}) caused by cavitation (Khmelev *et al.* 2014a) can be approximated by (30):

$$K \sim C(f)(I - I_0). \quad (30)$$

In expression (29) and (30) I_0 is threshold intensity which is necessary for cavitation appearing, W/m^2; ρ is density of liquid, kg/m^3; A is amplitude of oscillations, m; ω is angle frequency, s^{-1}; f is oscillations frequency, Hz; c is sound speed in liquid, m/s; h is layer thickness of liquid, m.

The variable h_1 in (29) is calculated by

$$h_1{}^2 = \frac{2cI_0}{\rho\omega^4 A^2}.$$

The proportionality coefficient in (30) can be estimated as inversely to f^3:

$$C(f) \sim \frac{1}{f^3}. \quad (31)$$

The proportionality can be explained in the following way. The maximum radius of cavitation bubble at the similar sound pressure is inversely to f, because then higher f, then lower time of bubble expansion. However the work of gas in the bubble during expansion is proportional to volume of bubble, which is determined as $\frac{4}{3}\pi R^3$. Thus, the energy spent to cavitation is inversely to f^3.

The obtained approximate dependences of US oscillations power spent for capillary waves formation are shown in Fig. 10.

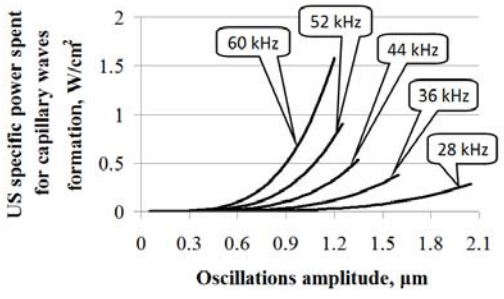

Fig. 10. Dependences of US specific power spent for capillary waves formation on oscillations amplitude at different frequencies.

As follows from presented dependences the increasing of oscillations amplitude and increasing of frequency causes to avalanche increasing of required US power and, consequently US power consumed by US radiator. For example, required power at 60 kHz 6 times more than power at 28 kHz. However the increasing of productivity at 60 kHz 1.11 times more than increasing at 28 kHz (see Fig. 8).

This shows appropriateness of using lower frequencies for absorption intensification, when small deviations of productivity are not critical.

5. CONCLUSION

Thus, the model of acoustic cavitation absorption intensification was developed. Analysis of the model has shown, that acoustic cavitation influence leads to the generation of capillary wave and consequently to the growth of surface of phase contact up to 3 times. It accelerates of gaseous mixture component mass transfer into liquid phase and consequently increases absorption productivity. For maximum absorption productivity increasing, the optimum modes of ultrasonic action are evaluated. It is shown, that the most appropriate frequency of ultrasonic vibrations is 60 kHz at amplitudes no more than 1.2 μm, at which more than 3 times increase of contact surface and more than 2 times increase of absorption productivity. Herewith, the liquid phase viscosity growing leads to increasing amplitudes which is necessary for achievement of defined productivity. And decreasing of surface tension leads to the decreasing amplitudes, which are necessary to defined productivity achievement, and the decreasing maximum amplitude providing capillary waves stability (no breakup into drops).

Obtained new scientific results have fundamental interest for the understanding of physical mechanism of the absorption acoustic cavitation intensification and they can be used for development of high-efficiency absorption apparatus that is supplemented by ultrasonic influence sources.

ACKNOWLEDGEMENTS

The reported study was supported by Grant of President of Russian Federation No. MK-4515.2016.8.

REFERENCES

Amin, R., A. Islam, R. Islam and S. Islam (2014). Simulation of N_2 Gas Separation Process from Air, *IOSR Journal of Applied Chemistry* 6(5), 9-13.

Brennen, C. E. (1995). *Cavitation and bubble dynamics*. Oxford University Press, United Kingdom.

Ho, M. T., G. W. Allinson and D. E. Wiley (2008). Reducing the cost of CO2 capture from flue gases using pressure swing adsorption, *Ind. Eng. Chem. Res.* 47(14), 4883-4890.

Kedrinsky, V. K. (2000). *Hydrodynamics of explosion. Experiment and models*, Publisher

of SB RAS, Novosibrisk, Russia. In Russian.

Khmelev, V. N., R. N. Golykh, A. V. Shalunov, A. V. Shalunova and D. V. Genne (2012). Revelation of optimum modes of ultrasonic influence for atomization of viscous liquids by mathematical modeling, *Proc. 13th International Conference and Seminar on Micro / Nanotechnologies and Electron Devices, EDM'2012*, Novosibirsk, Russia 114-123.

Khmelev, V. N., R. N. Golykh, A. V. Shalunov, S. S. Khmelev and K. A. Karzakova (2014a). Determination of ultrasonic effect mode providing formation of cavitation area in high-viscous and non-newtonian liquids, *International Conference of Young Specialists on Micro / Nanotechnologies and Electron Devices, EDM'2014*, Novosibirsk, Russia 203-207.

Khmelev, V. N., R. N. Golykh, A. V. Shalunov, V. A. Nesterov, A. V. Shalunova and E. V. Ilchenko (2014b). The study of process of cavitation bubbles interaction with interface boundary "liquid-gas" for evaluation of optimum modes providing maximum increasing of phases contact surface, *Science and technical bulletin of Volga region* 6, 362-364.

Khmelev, V. N., R. N. Golykh, S. S. Khmelev and R. V. Barsukov (2011). Method for Calculation of Optimum Intensity of Cavitation Influence on Viscous and Fine-dispersed Liquid Media, *Proc. 12th International Conference and Seminar on Micro / Nanotechnologies and Electron Devices, EDM'2011*, Novosibirsk, Russia, 245-250.

Konikoff, J. J. (1961). Oxygen recovery systems for manned space flight, *Aerospace Medicine* 701-712.

Laugier, F., C. Andriantsiferana, A. M. Wilhelm, and H. Delmas (2008). Ultrasound in gas-liquid systems: Effects on solubility and mass transfer, *Ultrasonics Sonochemistry* 15(6), 965-972.

Magaletti, F., L. Marino and C. M. Casciola (2015a). Diffuse interface modeling of a radial vapor bubble collapse, *Journal of Physics Conference Series* 656(1), 012028.

Magaletti, F., M. Gallo, L. Marino and C. M. Casciola (2015b). Dynamics of a vapor nanobubble collapsing near a solid boundary, *Journal of Physics Conference Series*, 656(1), 012012.

Magaletti, F., M. Gallo, L. Marino and C. M. Casciola (2016). Shock-induced collapse of a vapor nanobubble near solid boundaries, *International Journal of Multiphase Flow* 84, 34-45.

Margulis, M. A. and I. M. Margulis (2007). Dynamics of bubbles ensemble in cavitating liquid, *Physical chemistry journal* 81(12), 2290-2295.

McNeil, B. A., E. W. Scharpf and D. G. Winter (2000). *Integrated cryogenic and non-cryogenic gas mixture separation,* Patent US 6(161), 397 A.

Mulder, J. (1996). *Basic principles of membrane technology*, 2nd edition, Springer, Netherlands.

Rostrup-Nielsen, J.R. and J. Sehested (2003). Steam reforming for hydrogen. The process and the mechanism, *Fuel Chemistry Division Preprints* 48(1), 218-219.

Rozenberg, L. D. (1968). *Powerful ultrasonic fields*, Science, Moscow, Russia.

Rozhdestvensky, V. V. (1977). *Cavitation*, Shipbuilding, Leningrad, Russia.

Ruckenstein, E. and B. Nowakowski (1990). A Kinetic Theory of Nucleation in Liquids, *Journal of Colloid and Interface Science* 137(2), 583-592.

Scholes, C. A., C. J. Anderson, G. W. Stevens and S. E. Kentish (2013). Membrane Gas Separation–Physical Solvent Absorption Combined Plant Simulations for Pre-combustion Capture, *GHGT-11 Proceedings of the 11th International Conference on Greenhouse Gas Control Technologies*, Kyoto, Japan.

Sheng, C. and X. Shen (2006). Modelling of acoustic agglomeration processes using the direct simulation Monte Carlo method, *Journal of Aerosol Science* 1(37), 16-36.

Znyatdinova, L. R., Y. F. Korotkov, N. A. Nikolaev, A. A. Ovchinnikov, I. S. Dokuchaeva and A. N. Nikolaev (2010). *Vorticity atomizing absorber*, Patent RU 2,380,143 C2